sustainability

MDPI

Article

Climate-Based Analysis for the Potential Use of Coconut Oil as Phase Change Material in Buildings

Cibele Eller [1], Mohamad Rida [2], Katharina Boudier [2], Caio Otoni [3], Gabriela Celani [1], Lucila Labaki [1] and Sabine Hoffmann [2,*]

[1] Department of Architecture and Construction, University of Campinas (UNICAMP), Rua Saturnino de Brito, 224, Campinas 13083-889, SP, Brazil; cibeleeller@gmail.com (C.E.); celani@unicamp.br (G.C.); lucila@fec.unicamp.br (L.L.)
[2] Department of Civil Engineering, Technische Universität Kaiserslautern, Gebäude 14, Paul-Ehrlich-Straße, 67663 Kaiserslautern, Germany; r.mohamad1987@gmail.com (M.R.); katharina.boudier@gmail.com (K.B.)
[3] Institute of Chemistry, University of Campinas (UNICAMP), P.O. Box 6154, Campinas 13083-970, SP, Brazil; caio.otoni@ufscar.br
* Correspondence: sabine.hoffmann@bauing.uni-kl.de; Tel.: +49-(0)-631-205-2909

Abstract: One of the most efficient measures to reduce energy consumption in buildings is using passive thermal comfort strategies. This paper shows the potential of coconut oil as a bio-based phase change material (PCM) incorporated into construction components to improve the thermal performance of buildings for several climates, due to its environmental advantages, wide availability, and economic feasibility. The thermophysical properties of coconut oil were determined through differential scanning calorimetry. Numerical simulations were conducted in ESP-r, comparing an office space with a gypsum ceiling to one with coconut oil as PCM for 12 climate types in the Köppen–Geiger classification. The results show that coconut oil is a suitable PCM for construction applications under tropical and subtropical climates. This PCM can provide year-round benefits for these climates, even though a higher melting point is needed for optimum performance during hotter months. The highest demand reduction of 32% and a maximum temperature reduction of 3.7 °C were found in Mansa, Zambia (Cwa climate). The best results occur when average outdoor temperatures are within the temperature range of phase change. The higher the diurnal temperature range, the better the results. Our findings contribute to a better understanding of coconut oil in terms of its properties and potential for application in the building sector as PCM.

Keywords: phase change material; coconut oil; climate; thermal performance; building simulation

check for updates

Citation: Eller, C.; Rida, M.; Boudier, K.; Otoni, C.; Celani, G.; Labaki, L.; Hoffmann, S. Climate-Based Analysis for the Potential Use of Coconut Oil as Phase Change Material in Buildings. *Sustainability* **2021**, *13*, 10731. https://doi.org/10.3390/su131910731

Academic Editors: Nikos A. Salingaros, Alexandros A. Lavdas, Michael W. Mehaffy and Ann Sussman

Received: 15 July 2021
Accepted: 23 September 2021
Published: 27 September 2021

Publisher's Note: MDPI stays neutral with regard to jurisdictional claims in published maps and institutional affiliations.

1. Introduction

It is known that the way to mitigate the current process of climate change on our planet is a radical reduction in greenhouse gas emissions, which can be done by dramatically reducing energy consumption and shifting to more sustainable energy sources. According to the UN Global Status Report [1], the construction and operation of buildings together account for 39% of energy-related carbon dioxide emissions. Moreover, the operation of a building over its life is responsible for more than 80% of its carbon footprint.

The energy spent in air conditioning has globally doubled since 2000 despite the increase in the energy efficiency of HVAC equipment. Additionally, cooling demands are expected to grow quickly in developing countries, due to global warming and increasing urbanization rates [2,3]. High-rise office buildings that have been built with fully glazed façades and suspended ceilings since the 1960s, even when built with concrete, behave as a lightweight construction and usually rely on air conditioning for thermal comfort, which results in high energy consumption. There is, therefore, a need to find alternative thermal comfort strategies for retrofitting existing and new buildings with passive solutions.

Phase change materials (PCM) can compensate for the lack of thermal mass without overloading the building structure [4–6]. They act as added thermal mass to the building construction, working as thermal energy storage (TES) [6,7]. PCM absorb heat over the daytime and can reduce indoor temperature fluctuations due to their latent heat storage capacity [8,9]. The material stores latent heat during melting (endothermic phase transition), typically when temperatures increase during the day, and discharges the stored heat during solidification (exothermic phase transition), when temperatures decrease at night [10].

For several decades, phase change materials have been used in the building context in different applications, such as walls, ceilings, floors, and other building components, as well as heat and cold storage units [11]. Al-Yasiri and Szabó [12] summarized the results of recent studies for building envelopes with PCM and found that, depending on the PCM type, the location, and the incorporation method, indoor temperatures can be reduced from 2 °C to 7 °C; energy savings can range from 1.94% to 34%; cooling loads can be reduced from 9% to 73%; comfort hours can increase from 12% to 65%; and CO_2 emissions can be reduced up to 4817.44 kg/year (in one study that presented this datum). Additionally, transparent PCMs can be used in window cavities and decorative walls [5,9,13,14]. Gao et al. [14] integrated a 3 mm PCM to a double-pane window, saving up to 17.2% energy for HVAC systems and 9.4% energy for the whole building in a warm climate. Many materials can work as PCM. Nevertheless, for building purposes, the melting range of the PCM should stay close to the comfort zone. Tauseef-ur-Rehman et al. [15] suggest that this range should be between 18 and 30 °C. Since acceptable comfort limits vary from climate to climate, PCM properties should also vary by climate. Furthermore, increased nighttime ventilation has been proven to enhance the PCM performance, as it reinforces the rate of heat discharge and allows the solidification and melting cycle to continue [16].

Since PCM works by changing phases, generally from solid to liquid and from liquid to solid, it is important to consider an encapsulation method that can contain the product in its liquid state. A distinction is made between micro- and macro-encapsulated PCM materials. The micro-encapsulated PCM needs a carrier material such as plaster [17], whereas the macro-encapsulated material is stored in so-called containers [18].

Although PCMs have long been used to shift the effects of heating and cooling, they are not often used in developing countries and tropical climates. This is due not only to the high cost of the commercially available PCM products but also to their relatively low melting temperature since most of these are designed for colder climates [19]. Recently, coconut oil has been introduced as an inexpensive alternative PCM in Bandung, Indonesia [20,21].

Coconut Oil as PCM

Paraffin is currently the most commonly used PCM in the construction sector. Even though its application is mainly targeted towards improving thermal comfort and reducing energy consumption, paraffin is a product derived from petroleum, which is a fossil-based non-renewable resource. For this reason, researchers are exploring alternatives that are more environmentally friendly.

Chauhan et al. [22] point to the increasing interest in PCM based on vegetable oils such as coconut, palm, and soybean oils. These materials can operate in desired temperatures for construction applications and remain thermally stable for many years [22,23]. Moreover, vegetable oils are a natural and rapidly renewable resource with low embodied energy and are non-toxic and biodegradable [24]. Among these three, coconut oil stands out for the highest content of saturated fatty acids.

Although susceptible to rancidification to a higher or lesser extent, oils and fats benefit from prevented rancidity development as far as shelf life is concerned. Coconut oil is, per se, less prone to the major mechanisms of rancidification compared to other vegetable oils. First, the highly saturated nature of the fatty acids present in coconut oil renders it highly stable against oxidative rancidity, which is further prevented by limiting access to atmospheric oxygen and light by airtight encapsulation within high oxygen-barrier, opaque containers. Hydrolytic rancidity, in turn, is widely prevented in coconut oil owing to its extremely low moisture content (lower than 1%), besides presenting extremely low hygroscopicity and being encapsulated in high moisture-barrier containers. Finally, the low water activity is also key to avoiding microbial rancidity, which can be further reduced by pasteurization or, similar to the other mechanisms, the addition of small amounts of antioxidant compounds. All in all, the herein proposed solution can be non-speculatively claimed to boast extremely high stability against rancidification [25,26].

According to Kahwaji and White [27], coconut oil proved to be a feasible PCM for thermal energy storage. It has a latent heat of fusion of 105 ± 11 J/g, a low degree of supercooling, and a transition temperature ideal for applications in buildings (24.5 ± 1.5 °C), and it remained thermally stable after the melt–freeze cycles of the experiment. According to the authors, coconut oil can also be less expensive than other PCM products. Since coconut oil is widely available in tropical areas, this is a promising alternative to industrial PCM materials made for temperate climates.

Similar data were used by Wonorahardjo et al. [25], incorporating coconut oil into a room in Bandung, Indonesia. In this study, the PCM contributed to cooling the building during the day by reducing temperature peaks. The authors pointed to the need for good air circulation, so that the thermal mass effect can occur.

Other studies show that coconut oil can be used with other materials and encapsulation methods or with additives that improve its performance. Khamooshi and Khani [28] studied a building material made of coconut oil and expanded vermiculite, and the findings were all satisfactory for physical, mechanical, chemical, and thermal properties. Wi et al. [29] combined coconut and palm oils with exfoliated graphite nanoplatelets and were able to improve the thermal conductivity by over 400%.

Jeon et al. [30] studied the influence of coconut oil impregnated biochar that is produced out of waste material from pine cone, sawdust, and paper mill sludge as latent heat storage insulation. Alqahtani et al. experimentally and numerically explored the use of coconut oil as a phase change material in the building envelope in an unconditioned building for semi-arid regions [6]. The results showed a reduction of 5.2 °C for the indoor temperature while using coconut oil for the wall structure. By also implementing coconut oil in the window construction, a reduction of 7.2 °C was possible. There are still a few studies about coconut oil as PCM for possible applications in buildings. Nonetheless, the recent dates of the papers indicate that this is a current subject, and the positive findings suggest the potential that this material has as thermal energy storage for buildings.

While many PCM studies focus on finding the best product for a specific case and climate, this study is a simulation-based investigation of the potential of coconut oil as a year-round solution for different climate types. The aim is to identify the types of climates in which coconut oil, when applied to building components, will be most conducive to reducing indoor temperature peaks and energy consumption. The process analyzes the performance of the material applied to an office space and compares the results with climatic variables of each climate. The correlation between climate types and PCM selection is a valuable outcome, not only for the case of coconut oil but for other PCMs as well.

2. Materials and Methods

This research consists of a numerical simulation study in ESP-r to analyze the performance of coconut oil as PCM for different cities representing 12 climate types. One office space is modelled, and two different ceiling materials are compared: a typical suspended gypsum ceiling and a macro-encapsulated board containing coconut oil. To assess the performance of coconut oil as PCM, the following steps were defined, as in Figure 1:

- Selection of representative climates throughout the world.
- Characterization of the coconut oil sample through differential scanning calorimetry (DSC) measurements and modelling in ESP-r as PCM.
- Definition of a simulation model (geometry, materials, and schedules) of the office space.
- Definition of the metrics to evaluate the performance of the material.

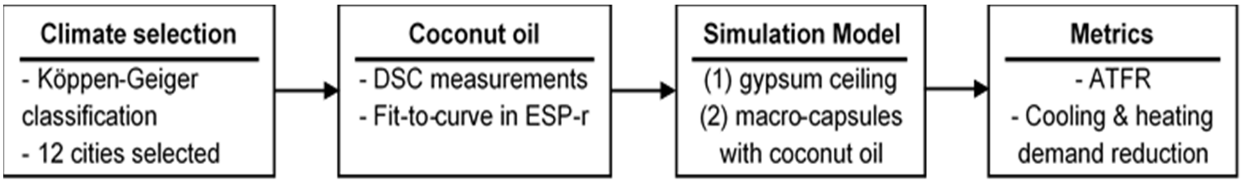

Figure 1. Methodology scheme of the presented study.

2.1. Climate Classification and Selection

The Köppen–Geiger classification is widely used to define different climate types around the world. The system consists of a three-letter classification and a total of 31 distinct climate types. The criteria to differentiate the climate take into account the annual and monthly mean temperatures (Tann, Tmax, Tmin), annual and monthly precipitation (Pann, Pmax, Pmin), and a dryness threshold (Pth) that is dependent on the annual mean temperature and the season in which the most precipitation occurs [31].

The first letter defines the broader groups of climates that are originally based on five different vegetation groups: (A) for equatorial climates, (B) for arid climates, (C) for warm temperate climates, (D) for snow climates, and (E) for polar climates. The second letter subdivides these five groups based on precipitation. The letter (s) means dry summer, (w) dry winter, and (f) fully humid. The third letter determines additional temperature conditions, with (a) to (d) ranging from hot to cold summers for (C) and (D) climates, and (h) for hot and (k) for cold in (B) climates [31]. Figure 2 shows a world map with the different climate types in the Köppen–Geiger classification [32].

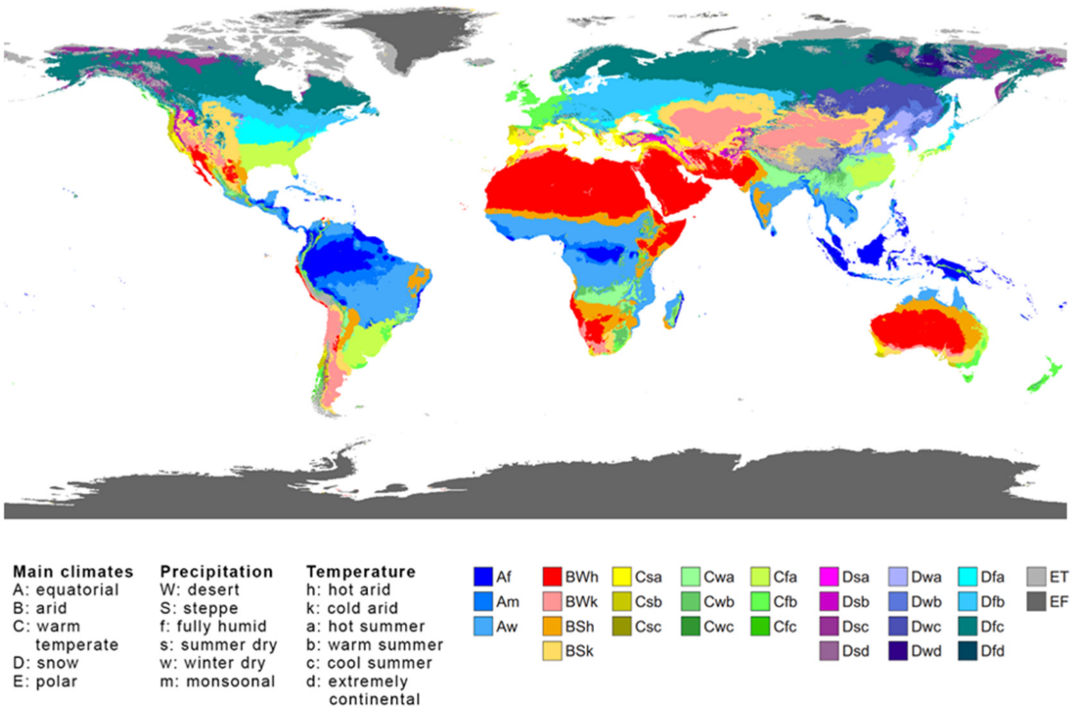

Figure 2. World map of Köppen–Geiger climate classification, adapted from [32].

For this research, we narrowed down the 31 different climates to 10 representative types of climates, according to Richards et al. [33]. Then, we subdivided the subtropical classification into three to analyze in more detail, since the annual average temperature of this group is closer to the melting and solidification temperatures of coconut oil. Table 1 shows the 12 selected cities, their climate classification, and the annual average temperature and diurnal temperature range for each of them.

Table 1. Representative climates, selected cities, and climatic conditions.

Representative Climates * (Köppen–Geiger Classification)	Chosen City	Country	Hemisphere	Climate	Average Temp. [°C]	Average Diurnal Temp. Range [K]
Tropical Rainforest (Af)	Bandung	Indonesia	Southern	Af	22.63	9.29
Tropical Monsoon (Am)	Cairns	Australia	Southern	Am	24.34	7.20
Savanna (Aw)	Dar Es Salaam	Tanzania	Southern	Aw	25.62	8.27
Hot Desert or Arid (BWh, BSh)	Karachi	Pakistan	Northern	BWh	26.46	9.80
Cold Desert or Arid (BWk, BSk)	Tehran	Iran	Northern	BSk	17.20	9.49
Mediterranean (Csa, Csb, Csc)	San Francisco	United States	Northern	Csb	13.78	7.91
Subtropical (Cwa, Cwb, Cwc, Cfa)	Mansa	Zambia	Southern	Cwa	18.54	13.48
	Campinas	Brazil	Southern	Cfa	22.03	11.70
	Guatemala City	Guatemala	Northern	Cwb	18.70	9.15
Oceanic (Cfb, Cfc)	London	United Kingdom	Northern	Cfb	11.99	6.03
Hot or Warm Continental (Dsa, Dsb, Dwa, Dwb, Dfa, Dfb)	Seoul	South Korea	Northern	Dwa	12.68	7.58
Cold Continental (Dsc, Dsd, Dwc, Dwd, Dfc, Dfd)	Fairbanks-Alaska	United States	Northern	Dfc	−1.52	10.01

* Reference: Richards et al., 2019 [33].

An important climatic aspect to be considered for PCM application is the diurnal temperature range (DTR), defined by the difference between the maximum and minimum temperatures that occur during one day. As a passive strategy, the PCM relies on the variation of ambient air temperature to be charged or discharged (i.e., to absorb or release latent heat). The temperature inside a room should vary enough along 24 h to melt and solidify the PCM.

2.2. Characterization of Coconut Oil through DSC

The sensible and latent heat of the coconut oil were measured through differential scanning calorimetry (DSC) with constant heating and cooling rate of 1 [K/min] (Table 2). The sample used was composed of 2/3 coconut oil and 1/3 sodium benzoate, in order to reduce the gap between solidification and melting temperatures. The peak temperature in the melting process was reached at 25 °C. The phase change process occurred over a temperature range of 9 K. Beyond the phase change, the heat capacity of the coconut oil was equal to 4.28 [kJ/kg K] in the solid phase and 2.45 [kJ/kg K] in the liquid phase. Table 2 presents the thermal properties of the sample. The thermal conductivity values were obtained from the literature using coconut oil data, since the influence of sodium benzoate was considered irrelevant for this study [34].

Table 2. Thermo-physical properties of coconut oil determined through DSC measurements in this study.

T Solid [°C]	T Liquid [°C]	Thermal Conductivity [W/mK] [34]		Specific Heat in the Solid Phase [kJ/kg K]		Latent Heat [kJ/kg]
		Solid Phase	Liquid Phase	Solid Phase	Liquid Phase	
16	25	0.32	0.80	4.28	2.45	64.59

The latent heat value from the DSC measurement is 64.59 [kJ/kg]. This is relatively low compared to other materials, such as paraffin, and to the coconut oil data that were used in other studies. Al-Jethelah et al. [35], Aloimair et al. [36], and Ebadi et al. [37] use the same data set in which coconut oil presents a latent heat of 103 [kJ/kg], which is similar to the above-mentioned study of Kahwaji and White [27].

2.3. Coconut Oil as PCM in ESP-r

To assess the potential of PCM to improve the thermal performance of buildings, ESP-r was selected as a simulation tool for this study. ESP-r is an open-source software that is well-known for its reliability and capability for predicting the thermal behavior of buildings [38]. Moreover, ESP-r is capable of modelling PCM integrated into building components [17]. The PCM module inside ESP-r allows for a detailed dynamic thermal characteristic of different PCMs inside building constructions [17]. Hoffmann and Kornadt [17] and other studies [8] showed that PCM modules in ESP-r yielded similar results compared to field studies.

In ESP-r, each construction layer is represented by three thermal nodes in the center of the layer, located at the outer surfaces and in the middle. All building energy modelling tools consider only rectangular shapes to represent the construction layers [18]. To allow for more detailed discretization in order to study the charging and discharging of PCM, 3D thermal modelling is used, which usually considers 3D finite element methods.

Rida and Hoffmann [18] investigated the influence of different PCM container geometry on the charge and discharge of the coconut oil in a ceiling application. By using a simulation method, they showed the relation between the heat transfer and the exposed surface area to the volume ratio of a macro-encapsulated PCM panel made of a thin plastic layer.

The heat transfer process in building structures containing PCM is complex, especially during the transition phase of the material. At any time during the simulation, PCM can be completely solid, completely liquid, or in transition (mushy state, wherein solid and liquid states coexist). In ESP-r, the phase change process is represented by a heat capacity method, in which the specific heat varies with temperature [17]. The PCM is applied to a layer within a multi-layer construction, and the nodes related to this layer are linked to a variable thermophysical property.

Henceforth, during the phase change, the total heat capacity $c(\theta)$ is given by Equation (1) [17]. The thermal energy $\dot{Q}$ that can be stored in a mass (m) of PCM during its phase change is described as a temperature-dependent heat capacity and the heat rate R in [K/s] [17].

$$\begin{cases} c(\theta) = c_{solid} & \theta < \theta_{solid} \\ c(\theta) = c_{solid} + c_{latent}(\theta) & \theta_{solid} < \theta < \theta_{liquid} \\ c(\theta) = c_{liquid} & \theta > \theta_{liquid} \end{cases} \quad (1)$$

$$\dot{Q}(\theta) = m\, c(\theta)\, R \quad (2)$$

There are two options to input the latent heat value of PCM in ESP-r. It can be a linear function or a curve. Based on the DSC measurements, we found that a fractional polynomial equation best fits the non-linear curve of the specific latent heat capacity

c_{latent} during the melting process (Figure 3). Equation (3) shows the fractional-polynomial equation used in ESP-r that corresponds to the method (SPMCPC55) [17].

$$c_{latent}(\theta) = \frac{a + c\theta + e\theta^2}{1 + b\theta + d\theta^2} \quad (3)$$

$$l = \int_{\theta_{solid}}^{\theta_i} c_{latent} d\theta \quad (4)$$

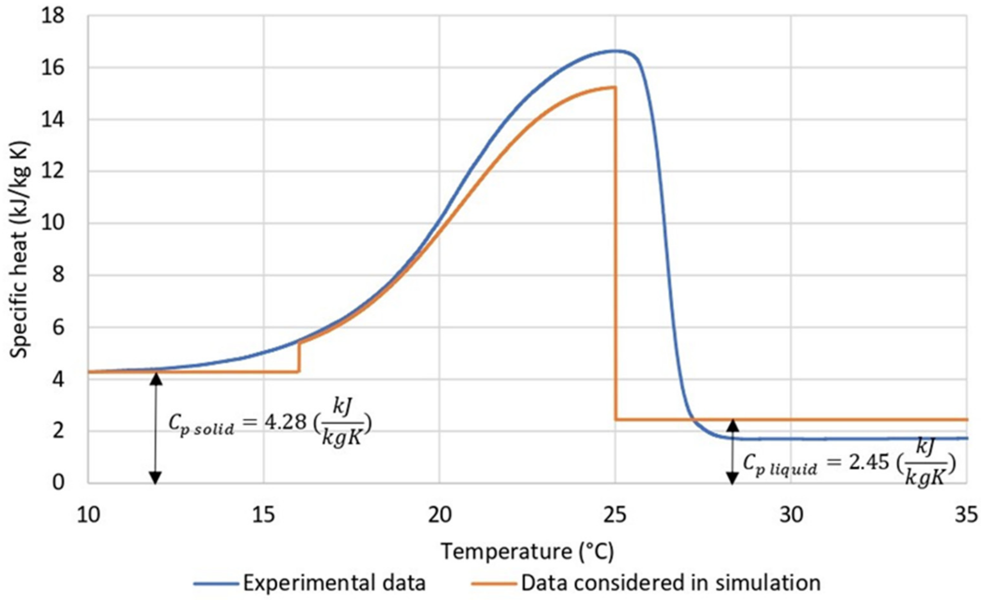

Figure 3. Specific heat curve of coconut oil derived from the DSC measurements (experimental data determined in this study) and the data considered for the simulation, based on the fit-to-curve method.

The coefficients (a), (b), (c), (d), and (e) for this study were found by applying a fit-to-curve method and are shown in Table 3. Figure 3 presents the experimental data derived from the DSC measurements and the data considered for the simulation with the fit-to-curve method and the fixed values for c_{solid} and c_{liquid}.

Table 3. Coefficients for the fit-to-curve method determined in this study.

Coefficient	Value
a	1250.8
b	−174.9
c	−0.0863
d	0.0020
e	6.6158

2.4. Simulation Model

As a prototypical room, one office space at an intermediate level of a high-rise building was modelled. The room dimensions are 8.0 m by 5.0 m, and the floor-to-ceiling height is 2.7 m (Figure 4). There is a glazed façade with a shading system/obstruction that decreases the solar load by 50%. The windows are facing the Equator, which is north for Southern Hemisphere cities and south for cities located in the Northern Hemisphere. The adjacent rooms are assumed to have similar temperatures to the base model, and for that, the internal walls, ceiling, and floor are set to have similar boundary conditions.

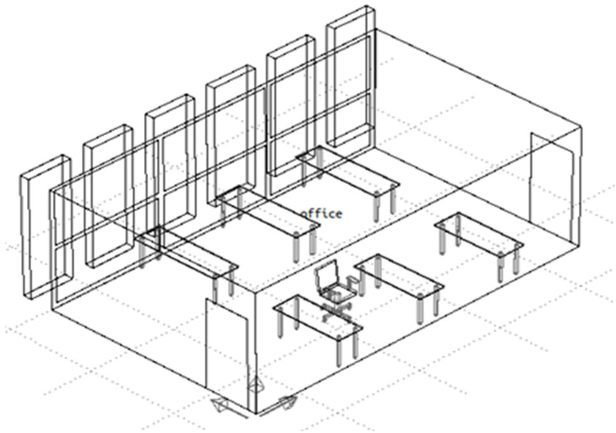

Figure 4. Prototypical office room.

The construction materials are presented in Table 4. They were selected based on a generic lightweight construction that is commonly used for office buildings. The same materials were considered for all 12 cases to reduce the number of variables and focus on PCM performance.

Table 4. Construction details of the building.

Construction	Layers (Outside to Inside)	U [W/m^{2}K]
Internal wall	White gypsum board (1.2 cm) Mineral wool (10 cm) White gypsum board (1.2 cm)	0.36
Single Glazing	Single glazing (0.6 cm)	5.69
Ceiling	Floor tiles (0.6 cm) Concrete slab (20 cm) Air Gap (50 cm) + Gypsum board (2 cm) (Base Case) or PCM (2 cm) (Coconut Oil)	1.89 (Base Case) 2.00 (PCM/Coconut Oil Case)
Floor	Concrete slab (20 cm) Floor tiles (0.6 cm)	3.5

The reference case has a typical suspended gypsum ceiling. In the second case, the gypsum ceiling is replaced by macro-encapsulated PCM panels containing coconut oil. The macro encapsulation of the PCM can be done using a variety of materials and methods. Yabuki [39], for example, uses vacuum forming to shape upcycled plastic into ceiling tiles filled with PCM, as seen in Figure 5. Since the encapsulation material is very thin, thus having an undermost influence on the heat transfer process, we did not consider it for the simulation. The PCM was modelled as two layers of 1 cm each on the ceiling, totaling a volume of 0.8 m^3 and 27% of surface area in the room.

Figure 5. Molded recycled plastic forms that act as PCM containers for ceiling construction [39].

Each layer in ESP-r has three nodes, one on each side and another in the middle. To increase the accuracy of the calculation, the 2 cm PCM layer is discretized into two layers of 1 cm each. This increases the number of nodes of the PCM layer from 3 to 5 nodes.

To account for natural ventilation, a fixed number of four air changes per hour has been defined during office hours and eight air changes per hour during the night. The increased nighttime ventilation is desirable to cool down the room and improve PCM performance. It is important to highlight that for result comparison by reducing the number of variables, these characteristics were replicated to all the analyzed climate types, even though ventilation patterns would vary. The casual internal gains were defined as 40.0 [W/m^2] for sensible heat and 16.5 [W/m^2] for latent heat, including occupants, lighting, and equipment, from 8 a.m. to 6 p.m.

Two simulation approaches were conducted to evaluate the suitability of coconut oil as PCM in different climates. The first one was simulated as a free-float space to calculate temperature reductions and the second one as an ideal control to observe the influence on cooling and heating demand.

For the simulations, we used weather files that consider typical meteorological years (TMY) and refer to real climate values of the last years. In addition to temperature, wind speed and direction, and humidity, these files also take into consideration the daylight illuminance and solar radiation and show whether the sky was overcast or clear.

2.4.1. Free-Float Space for ATFR and MTR

In the free-float model, indoor temperatures can fluctuate freely without any mechanical cooling or heating device, or other types of control. By using a free-float scenario in the simulation, it was possible to monitor the changes in indoor temperatures considering only natural ventilation. Operative temperatures were calculated based on air temperature in the room (fully mixed air with one temperature node in the middle) and the average surface temperature, which is the mean radiant temperature. The two models (with and without PCM) were simulated for each city. Operative temperatures of the room calculated through the simulations were then used to calculate the average temperature fluctuation reduction (ATFR) and the maximum temperature reduction (MTR).

ATFR is a metric that can estimate the monthly performance of the PCM [40]. Instead of using specific or typical days, it accounts for all temperatures throughout the year. ATFR is calculated by the average of the hourly difference between temperatures, comparing the models with and without PCM, as shown in Equation (5). In this study, we calculated the ATFR exclusively for office hours, on weekdays, from 8 a.m. to 6 p.m.

$$\text{ATFR} = \text{Average } \left| T_{NoPCM} - T_{PCM} \right| \quad (5)$$

MTR reveals the highest temperature decrease that occurs in the room on one specific day of the entire year. It can be calculated by Equation (6).

$$MTR = \text{Max}\,(T_{NoPCM} - T_{PCM}) \text{ if } (T_{NoPCM} - T_{PCM}) > 0 \quad (6)$$

2.4.2. Control Model for Heating and Cooling Demand

The second model has an added control system that regulates the temperatures inside the room, making it possible to calculate heating and cooling demand. We defined an ideal controller in ESP-r with a cooling setpoint at 26 °C and a heating setpoint at 20 °C. The control turns on during working hours, so the results in [kWh/year] refer to weekdays, from 8 a.m. to 6 p.m.

3. Results and Discussion

The thermal performance of the PCM in the free float model was evaluated in comparison with the climatic conditions for the selected cities. The graphs (Figures 6–10) are grouped by climate type and present the results for the reduction of cooling and heating demand (a) and the ATFR (b). As climate parameters, the monthly average temperatures (c) and diurnal temperature ranges (d) are also shown. The phase change range of coconut oil of 16–25 °C is highlighted in (c), corresponding to a temperature difference of 9 K, which is marked in the DTR graphs (d) for reference.

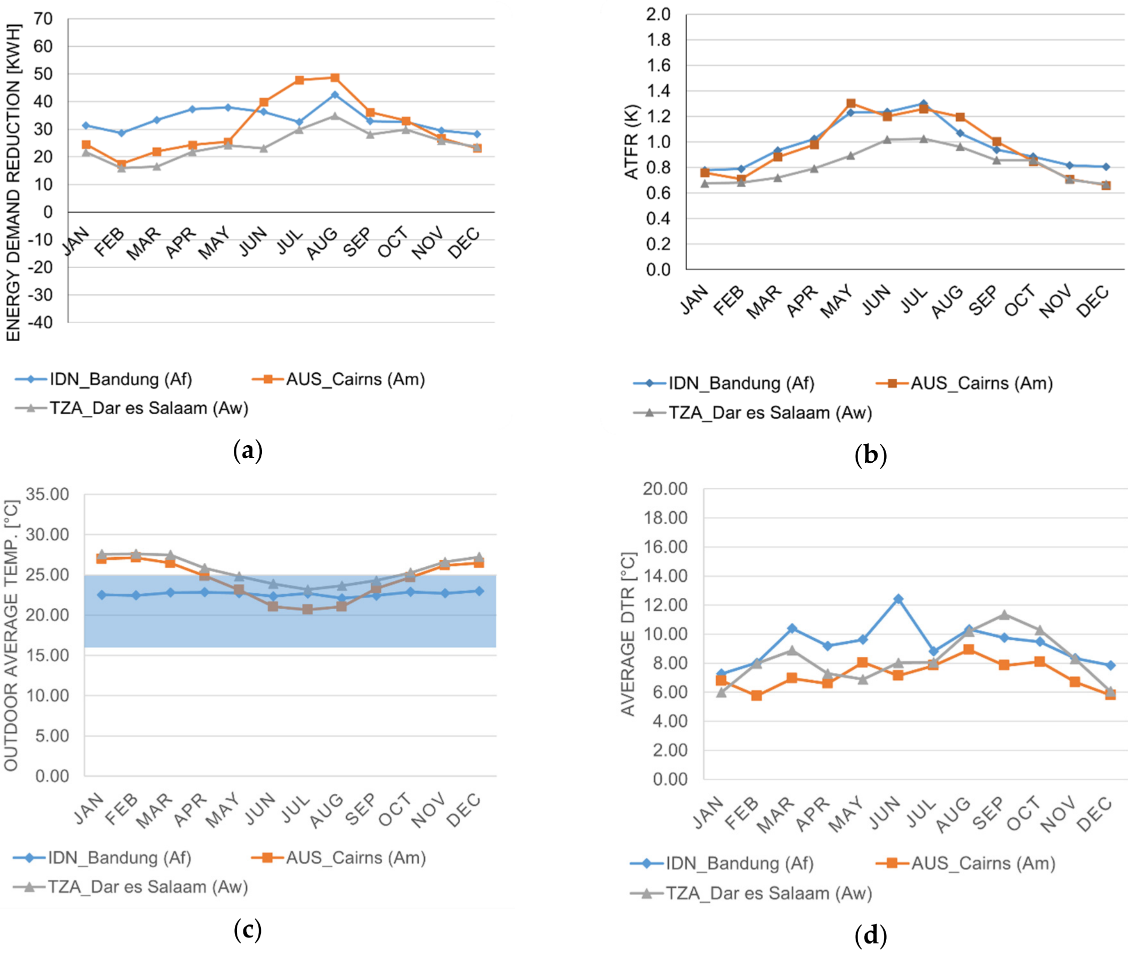

Figure 6. Results for type A climates. (**a**) Cooling and heating reduction. (**b**) Average temperature fluctuation reduction. (**c**) Outdoor average temperature. (**d**) Outdoor diurnal temperature range. The blue area in (**c**) is the transition range of the coconut oil.

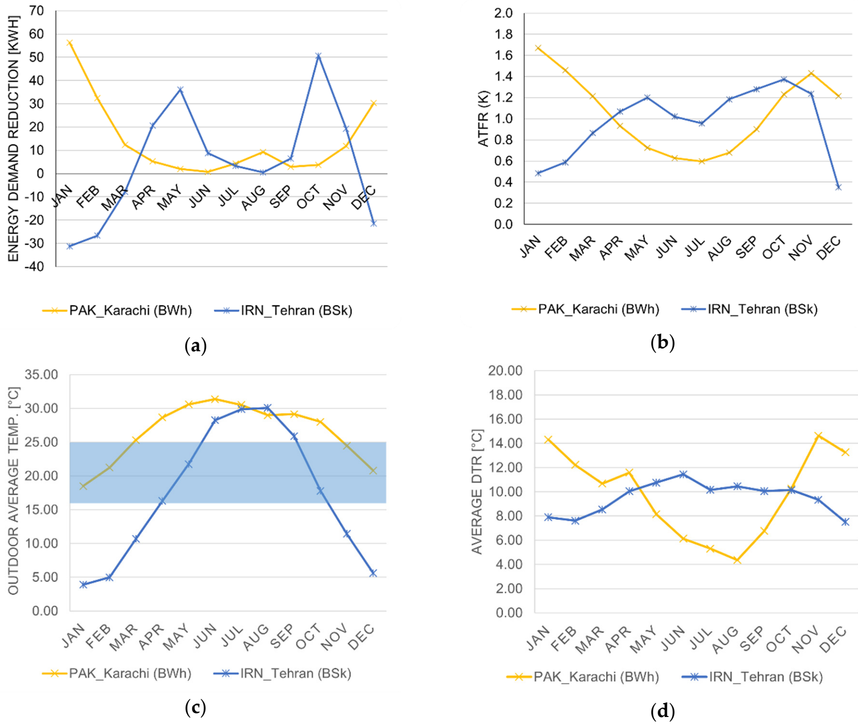

Figure 7. Results for type B climates. (**a**) Cooling and heating reduction. (**b**) Average temperature fluctuation reduction. (**c**) Outdoor average temperature. (**d**) Outdoor diurnal temperature range. The blue area in (**c**) is the transition range of the coconut oil.

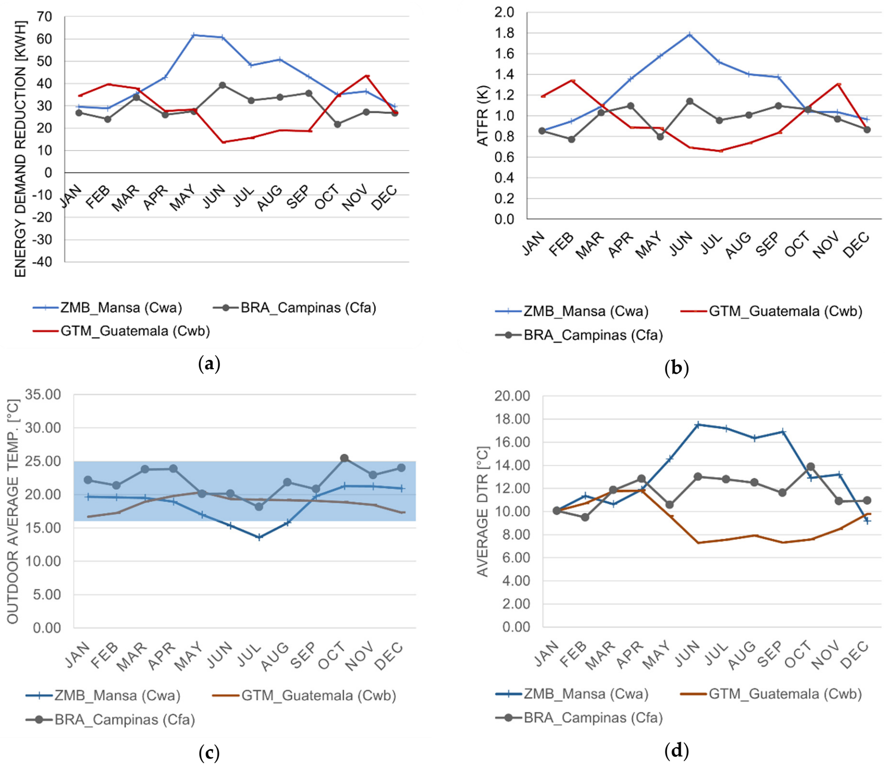

Figure 8. Results for type C climates. (**a**) Cooling and heating reduction. (**b**) Average temperature fluctuation reduction. (**c**) Outdoor average temperature. (**d**) Outdoor diurnal temperature range. The blue area in (**c**) is the transition range of the coconut oil.

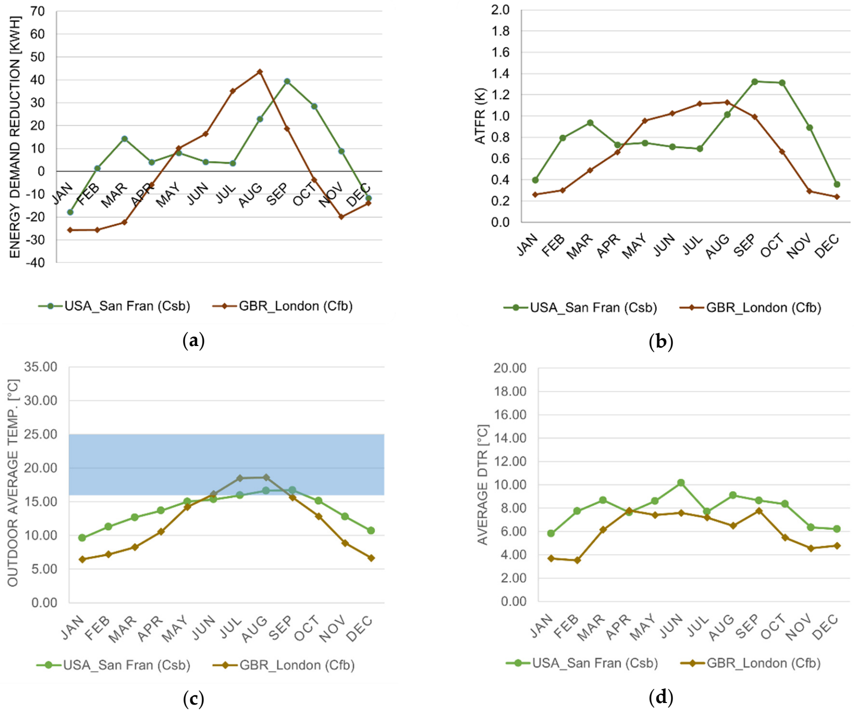

Figure 9. Results for type C climates other than subtropical. (**a**) Cooling and heating reduction. (**b**) Average temperature fluctuation reduction. (**c**) Outdoor average temperature. (**d**) Outdoor diurnal temperature range. The blue area in (**c**) is the transition range of the coconut oil.

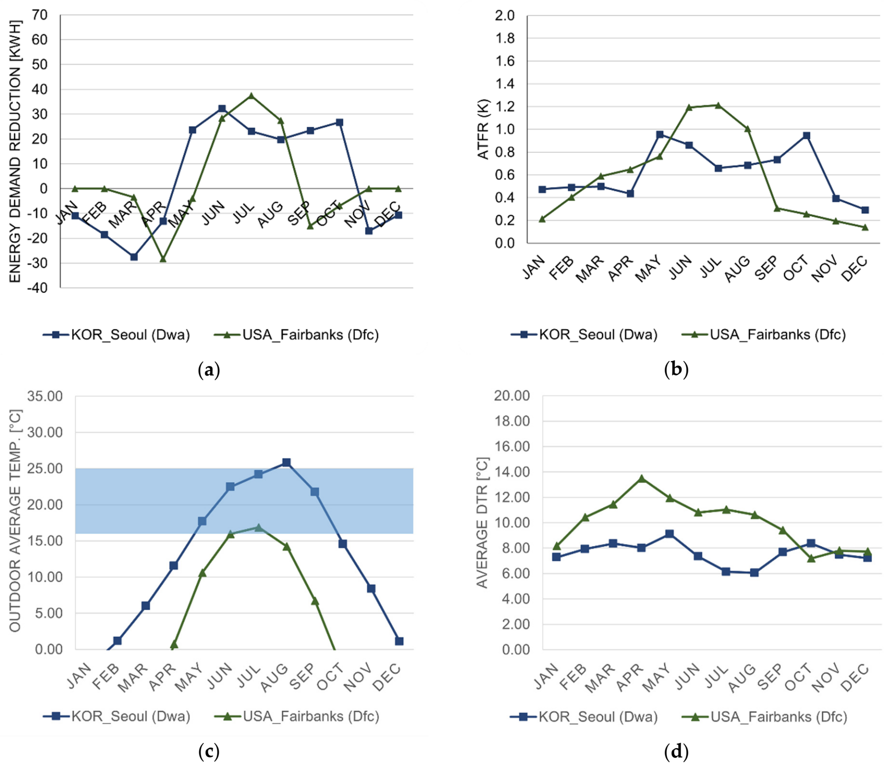

Figure 10. Results for type D climates. (**a**) Cooling and heating reduction. (**b**) Average temperature fluctuation reduction. (**c**) Outdoor average temperature. (**d**) Outdoor diurnal temperature range. The blue area in (**c**) is the transition range of the coconut oil.

3.1. Climates Type A and B

Type (A) climates present a year-round reduction in cooling and heating (Figure 6a). The ATFR results stay at a high range throughout the year, reaching as high as 1.3 K for Bandung and Cairns in May and July and as low as 0.7 K in December for Dar es Salaam and Cairns (Figure 6b). These are tropical climates with constant temperatures during the year that coincide with the upper portion of the coconut oil transition range (Figure 6c). The diurnal range varies between 6 and 11 K (Figure 6d).

Type (B) climates are primarily classified based on a dryness threshold and not on the average temperature, as in the case of the others. Thus, Figure 7c shows the differences in outdoor temperatures of Karachi, a hot desert, and Tehran, a cold steppe. In both cities, however, warm and cool seasons are clearly defined. The DTR varies differently for each case and has an impact on ATFR results (Figure 7d). Respectively, for Karachi and Tehran, the lowest ATFRs show 0.6 and 0.3 K, and the highest 1.7 and 1.4 K (Figure 7b). The energy reduction is higher when the temperatures are within the coconut oil range and lower in the extremes (Figure 7a).

3.2. Climates Type C

Type (C) climates were divided into two subcategories based on the similarities of the outdoor average temperatures and heating demand. The first, type (C) subtropical, presents relatively higher average temperatures and no active heating demand, compared to the second group, defined as type (C) other.

(C) subtropical climates show a large energy reduction (Figure 8a), and high ATFR is achieved in all the months of the year (Figure 8b). Like type (A) climates, the lowest ATFR value is only 0.7 K, registered in Guatemala in July. These are subtropical climates with average temperatures within the coconut oil temperature range (Figure 8c) and high DTR (Figure 8d). There is a peak of over 60 kWh and 1.8 K in Mansa in June, which is also the month with the highest diurnal temperature range.

Figure 9 shows the results for the other types of (C) climates. These two cities are colder than the (C) subtropical and display distinct warm and cold seasons. The DTR values are generally below 9 K (Figure 9d), and the ATFR results are more related to the average temperatures, which are lower during the winter and higher during summer or shoulder seasons (Figure 9c). The highest ATFR results respectively show 1.3 and 1.1 K for San Francisco and London, and the lowest 0.4 K and 0.2 K in December (Figure 9b). During heating-dominant seasons, there is an increase in energy demand (Figure 9a).

3.3. Climates Type D

Type (D) climates are much colder climates, presenting a winter season with snow. Energy reduction only occurs during the summer/fall (Figure 10a). The ATFR results display at the lower end of the graph during winter, reaching higher values during the summer and fall (Figure 10b). The values, however, only reach as high as 1.2 K in Fairbanks and 1.0 K in Seoul. Higher ATFRs in Seoul correspond to a higher DTR, whereas in Fairbanks they correspond to a higher average temperature. In this last case, ATFR is still affected by DTR, as can be seen comparing the months of April and October. They present comparable average temperatures, but ATFR is higher when DTR is also higher.

3.4. Overall Energy Reduction

Figure 11 presents the cooling and heating demands for the 12 cities using the control model. The cities and the mentioned abbreviations are listed in Table 5. It is possible to observe great discrepancies in terms of heating and cooling demands, which are expected since the climates are very different from one another. In general, tropical and hot desert climates will have higher cooling demands than temperate climates. Heating demands are found in cold desert, Mediterranean, oceanic, and continental climates (see Table 1 for reference).

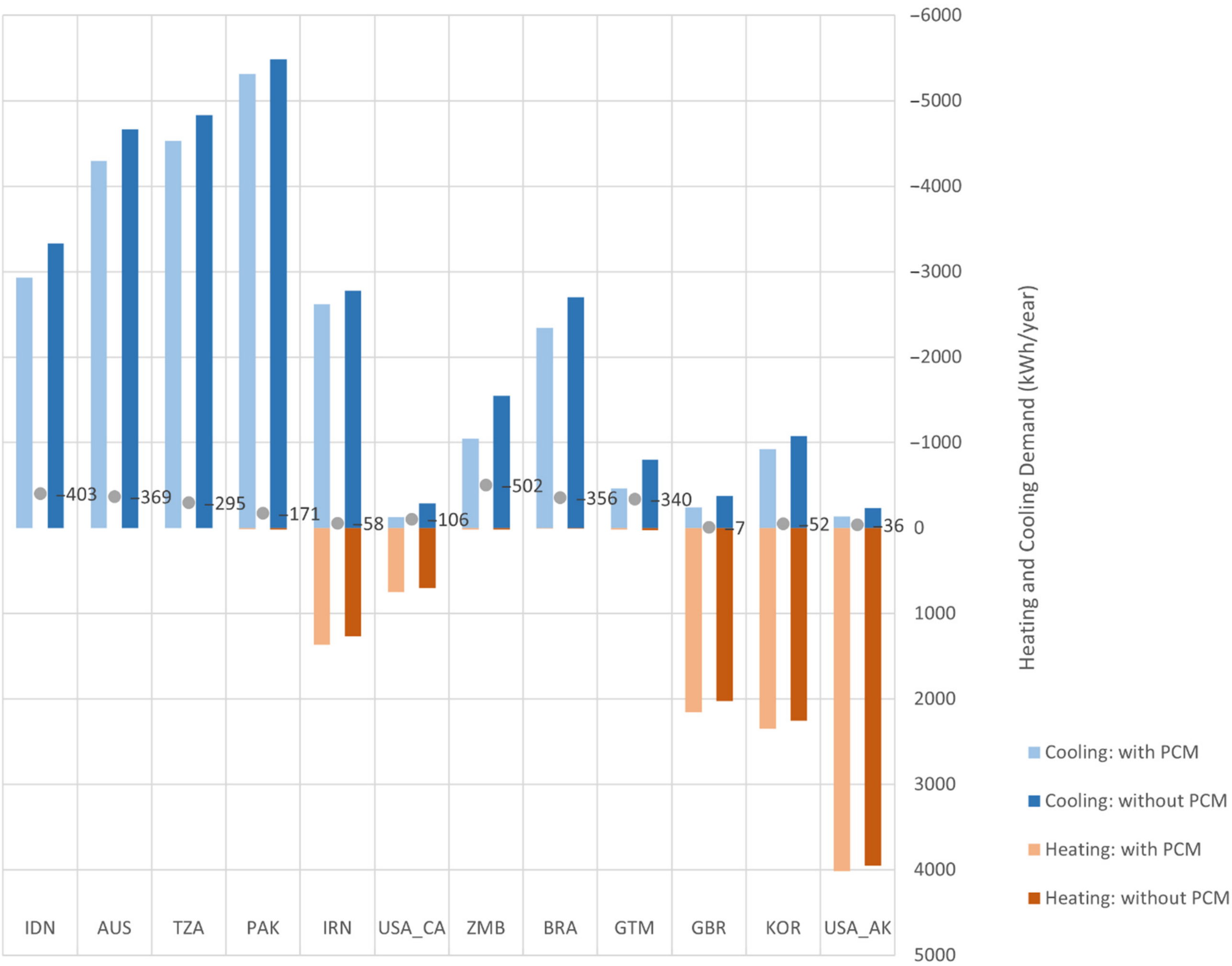

Figure 11. Cooling and heating demand for the 12 cities investigated herein.

Table 5. Cooling and heating demand reduction after PCM.

			Reduction in kWh/Year (NoPCM-withPCM)			% Overall Reduction C+H
#	**City**	**Climate**	**Cooling**	**Heating**	**C+H**	
1	ZMB_Mansa	Cwa	−499	−3	−502	32%
2	IDN_Bandung	Af	−403	0	−403	12%
3	AUS_Cairns	Am	−369	0	−369	8%
4	BRA_Campinas	Cfa	−355	−1	−356	13%
5	GTM_Guatemala	Cwb	−337	−3	−340	41%
6	TZA_Dar es Salaam	Aw	−295	0	−295	6%
7	PAK_Karachi	BWh	−169	−2	−171	3%
8	USA_CA_San Francisco	Csb	−156	+51	−106	11%
9	IRN_Tehran	BSk	−160	+101	−58	1%
10	KOR_Seoul	Dwa	−150	+98	−52	2%
11	USA_AK_Fairbanks	Dfc	−97	+62	−36	1%
12	GBR_London	Cfb	−136	+129	−7	0%

In most cases, energy reduction is presented in terms of percentage. In this case, however, we ranked the results by absolute values because we are dealing with very different climates (Table 5). For example, San Francisco and Bandung have similar reductions of 11% and 12%; however, the amount of energy reduction in the former is only 106 [kWh/year] compared to 403 [kWh/year] in the latter. The percentage reduction is also in Table 5, for reference.

The first six cities correspond to type (A) and type (C) subtropical climates, and there is on average a reduction of about 380 kWh in combined cooling and heating loads. The difference between the results of the sixth and seventh position is almost twice as low, and the same is true between the eighth and ninth positions. Analyzing the three color-coded groups, we noticed that even though the cooling demands are very different for each climate (Figure 11), the total amount saved with the use of coconut oil is in the same range for each group.

Coconut oil had a negative effect on the heating demand during office hours for the last five cities of the 12 listed in Table 5. As PCM tends to lower the temperatures during the day, it can cause an increase in the heating demand for cities that require active heating. Figure 12 exemplifies this phenomenon, showing the same days for (a) London and (b) Mansa. In London, the temperatures are reduced below the heating threshold, causing the heating demand to increase. In Mansa, on the other hand, this decrease aids in the cooling process by lowering the temperatures from roughly 28 °C to 26 °C. A shortcoming of the study is that it considers constant natural ventilation, even when temperatures are below the comfort zone.

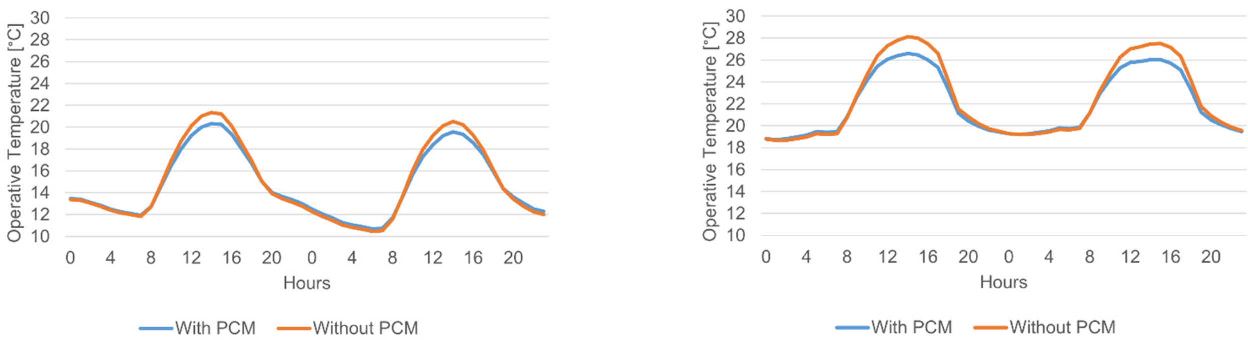

(**a**) London, GBR (**b**) Mansa, ZMB

Figure 12. Operative temperatures for March 1st and 2nd showing that PCM tends to lower the temperatures during office hours. (**a**) London, Great Britain. (**b**) Mansa, Zambia.

Cooling and heating demand reduction makes explicit the impact of heating dominant seasons on the performance of the PCM. Based on the results and the increase in heating demand, coconut oil is not recommended to be used in office buildings as PCM for climates that require active heating.

3.5. Overall ATFR and MTR

Table 6 shows the overall results for ATFR and MTR. ATFR results are similar for climates that either have high ATFR values throughout the year, such as types (A) and (C) subtropical, as well as climates that present high peaks, such as type (B). The five cities that presented improved results in energy demand reduction (Table 5) also have an ATFR of 1.0 K or higher.

Table 6. Average temperature fluctuation reduction and maximum temperature reduction in kelvin (K).

#	City	Climate	ATFR	MTR	Highest ATFR and MTR
1	ZMB_Mansa	Cwa	1.2	3.7	Winter
2	PAK_Karachi	BWh	1.1	3.7	Winter
3	IDN_Bandung	Af	1.0	2.3	Winter
4	BRA_Campinas	Cfa	1.0	2.5	Winter
5	IRN_Tehran	BSk	1.0	3.3	Fall
6	GTM_Guatemala	Cwb	1.0	3.1	Winter
7	AUS_Cairns	Am	1.0	2.3	Winter
8	USA_CA_San Francisco	Csb	0.8	3.3	Fall
9	TZA_Dar es Salaam	Aw	0.8	2.2	Winter
10	GBR_London	Cfb	0.7	3.1	Summer
11	KOR_Seoul	Dwa	0.6	3.0	Fall
12	USA_AK_Fairbanks	Dfc	0.6	3.1	Summer

The results for MTR range from 2.2 K in Dar es Salaam to 3.7 K in Mansa and Karachi. The highest MTR happens in the same season that the highest ATFR occurs, usually in the same month or one month apart. According to Table 6, the highest results take place during the winter in warmer climates and during the summer or fall in colder climates. The seasons are according to the meteorological definition that begins on the first day of the months that include solstices and equinoxes and are opposite for Northern and Southern Hemispheres.

All types of climates present high values of ATFR in specific months. The performance increases when the outdoor average temperature is within the coconut oil transition temperatures. This means that it decreases considerably during heating dominant seasons. There is also a decrease in ATFR values when the average temperatures substantially exceed the coconut oil transition range, as it can be observed for warmer months in type (B) climates. If the surface temperature at the PCM layer during a season is always higher than its melting point (in this case, 25 °C), the material will stay in the liquid phase and temporarily lose its phase change benefits.

There is a similarity between the graphs for ATFR and those for the diurnal temperature range. This suggests that within an acceptable average temperature range, the higher the DTR, the higher the ATFR. If the diurnal temperature range is much lower than the range of the PCM (in this case, 9 K), the material is not able to fully solidify during the night. However, even when DTR is not high enough, PCM can still work, not at its full capacity, but as partially melted and partially solidified.

4. Conclusions

A climate-based analysis was conducted assessing the effect of coconut oil in ceiling tiles to improve the thermal performance of commercial buildings. Simulations were made in a prototypical office room for 12 cities, representing climates under the Köppen–Geiger climate classification. The variables analyzed were energy demand reduction, average temperature fluctuation reduction, and maximum temperature reduction for each month of an entire year. Based on the results and discussion of this study, the outcomes are listed below:

1. Coconut oil can be used as a phase change material for the building sector, although its effectiveness correlates to the type of climate where it is applied.
2. The climate analysis showed improved performances mainly in type (A) tropical and type (C) subtropical climates, for which this material provides benefits throughout the year by reducing energy peaks and energy demand. Other climates have presented improved results, but only for specific periods of the year.

3. The room with PCM performs comparatively better when the outdoor average temperature is within the phase change range of the coconut oil. Within these limits, the higher the diurnal temperature range, the greater the results.
4. The highest ATFR occurred in summer/fall for colder climates and winter for warmer climates, which suggests that for the latter, coconut oil may have lower performance when temperatures are too high. In those cases, if summer optimization is desired, a higher melting point is recommended. Nonetheless, even without undergoing the phase change, the material is still beneficial since the heat capacity of coconut oil is higher than that of gypsum plaster.

Coconut trees grow in the climates that presented the best results. According to the Food and Agriculture Organization [41], the top five countries that produce coconut are Indonesia, the Philippines, India, Sri Lanka, and Brazil. This observation corroborates the hypothesis that coconut oil has great potential for the building sector as a more sustainable alternative.

Further work is still needed to develop construction materials that incorporate macro-encapsulated coconut oil at a reasonable cost, presenting high durability, safety, and design. Ideally, these products should be produced locally, using available materials and local labor, avoiding long-distance transportation, and contributing to the local economy. Future work may include full-scale experimental models, varying the position and amount of coconut oil, and incorporating adaptive comfort metrics. Moreover, further optimization of the coconut oil mix should be conducted in order to improve performance. Overall, the findings contribute to a better understanding of the material applied to buildings, and the process is helpful not only for coconut oil but also for the selection of other PCM for different climates.

Author Contributions: Conceptualization, C.E., G.C. and S.H.; methodology, C.E., M.R., K.B. and S.H.; software, M.R. and K.B.; validation, C.E., M.R. and S.H.; formal analysis, C.E.; investigation, C.E., M.R., K.B. and C.O.; resources, M.R., K.B. and C.O.; data curation C.E. and M.R.; writing—original draft preparation, C.E., M.R. and K.B.; writing—review and editing, C.E., M.R., K.B., G.C. and C.O.; visualization, C.E.; supervision, S.H. and L.L.; project administration, G.C. and S.H.; funding acquisition, G.C., S.H. and K.B. All authors have read and agreed to the published version of the manuscript.

Funding: This research was funded by the Brazilian-Germany Research Cooperation Scheme PROBRAL, a joint initiative of the "Coordenação de Aperfeiçoamento de Pessoal de Nível Superior-Brasil" (CAPES) and the German Academic Exchange Service (DAAD), grant number [0428/2019/88881.198752/2018-01]. Supported by the German Academic Exchange Service (DAAD) from funds of the Federal Ministry of Education and Research (BMBF).

Institutional Review Board Statement: Not applicable.

Informed Consent Statement: Not applicable.

Data Availability Statement: Not applicable.

Conflicts of Interest: The authors declare no conflict of interest.

Abbreviations

Abbreviation	Meaning
ATFR	Average temperature fluctuation reduction
DSC	Differential scanning calorimetry
DTR	Diurnal temperature range
ESP-r	Environmental Systems Performance-Research (name of the building simulation software)
HVAC	Heating ventilation air conditioning system

MTR	Maximum temperature reduction
PCM	Phase change material
Pann, Pmax, Pmin	Annual precipitation, max and min monthly precipitation
Pth	Dryness threshold
SPMCPC55	Method in ESP-r to consider PCM
Tann, Tmax, Tmin	Annual mean temperature, max and min monthly temperature
TES	Thermal energy storage
Mathematical abbreviations	
$c(\theta)$	Heat capacity
c_{latent}	Latent heat capacity
c_{liquid}	Liquid heat capacity
c_{solid}	Solid heat capacity
m	Mass
$\dot{Q}(\theta)$	Thermal energy
R	Heat rate
T_{NoPCM}	hourly temperature difference for the model without PCM
T_{PCM}	Hourly temperature difference for the model with PCM
Cities	
AUS	Cairns, Australia
BRA	Campinas, Brazil
GBR	London, Great Britain
GTM	Guatemala City, Guatemala
IDN	Bandung, Indonesia
IRN	Tehran, Iran
KOR	Seoul, South Korea
PAK	Karachi, Pakistan
TZA	Dar es Salaam, Tanzania
USA_AK	Fairbanks, Alaska, United States
USA_CA	San Francisco, California, United States
ZMB	Mansa, Zambia
Climate	
First letter	Defines the groups of climates based on five different vegetation groups
A	Equatorial climate
B	Arid climates
C	Warm temperate climates
D	Snow climates
E	Polar climates
Second letter	Divides the climate groups based on precipitation
s	Dry summer
w	Dry winter
f	Fully humid
Third letter	
a to d	Ranging from hot to cold summers (for C and D climates)
(h) and (k)	Hot and cold climates (in B climates)

References

1. UN Environment: Global Status Report 2018. Global Status Report: Towards a Zero-Emission, Efficient and Resilient Buildings and Construction Sector. Available online: https://www.unep.org/resources/report/global-status-report-2018 (accessed on 20 September 2021).
2. UN Environment: Emissions Gap Report 2018. Available online: https://www.unep.org/resources/emissions-gap-report-2018 (accessed on 20 September 2021).
3. Ichord, R.F. Urbanization and the Growing Demand for Cooling in a Warming Climate: Buildings as a Critical Resource. Atlantic Council. 3 July 2019. Available online: https://www.atlanticcouncil.org/blogs/energysource/urbanization-and-the-growing-demand-for-cooling-in-a-warming-climate-buildings-as-a-critical-resource/ (accessed on 20 September 2021).
4. Liu, Z.; Yu, Z.; Yang, T.; Qin, D.; Li, S.; Zhang, G.; Haghighat, F.; Joybari, M.M. A review on macro-encapsulated phase change material for building envelope applications. *Build. Environ.* **2018**, *144*, 281–294. [CrossRef]
5. Silva, T.; Vicente, R.; Rodrigues, F. Literature review on the use of phase change materials in glazing and shading solutions. *Renew. Sustain. Energy Rev.* **2016**, *53*, 515–535. [CrossRef]

6. Alqahtani, T.; Mellouli, S.; Bamasag, A.; Askri, F.; Phelan, P.E. Experimental and numerical assessment of using coconut oil as a phase-change material for unconditioned buildings. *Int. J. Energy Res.* **2020**, *44*, 5177–5196. [CrossRef]
7. Ben Romdhane, S.; Amamou, A.; Ben Khalifa, R.; Saïd, N.M.; Younsi, Z.; Jemni, A. A review on thermal energy storage using phase change materials in passive building applications. *J. Build. Eng.* **2020**, *32*, 101563. [CrossRef]
8. Kośny, J. *PCM-Enhanced Building Components. An Application of Phase Change Materials in Building Envelopes and Internal Structures. Engineering Materials and Processes*; Springer: Cham, Switzerland, 2015.
9. Ghalambaz, M.; Zadeh, S.M.H.; Mehryan, S.; Pop, I.; Wen, D. Analysis of melting behavior of PCMs in a cavity subject to a non-uniform magnetic field using a moving grid technique. *Appl. Math. Model.* **2020**, *77*, 1936–1953. [CrossRef]
10. Pielichowska, K.; Pielichowski, K. Phase change materials for thermal energy storage. *Prog. Mater. Sci.* **2014**, *65*, 67–123. [CrossRef]
11. Sharma, A.; Tyagi, V.V.; Chen, C.R.; Buddhi, D. Review on thermal energy storage with phase change materials and applications. *Renew. Sustain. Energy Rev.* **2009**, *13*, 318–345. [CrossRef]
12. Al-Yasiri, Q.; Szabó, H. Incorporation of phase change materials into building envelope for thermal comfort and energy saving: A comprehensive analysis. *J. Build. Eng.* **2020**, *36*, 102122. [CrossRef]
13. Fokaides, P.A.; Kylili, A.; Kalogirou, S.A. Phase change materials (PCMs) integrated into transparent building elements: A review. *Mater. Renew. Sustain. Energy* **2015**, *4*, 6. [CrossRef]
14. Gao, Y.Q.; Zheng, Q.; Jonsson, J.C.; Lubner, S.; Curcija, C.; Fernandes, L.; Kaur, S.; Kohler, C. Parametric study of solid-solid translucent phase change materials in building windows. *Appl. Energy* **2021**, *301*, 117467. [CrossRef]
15. Rehman, T.-U.; Ali, H.M.; Janjua, M.M.; Sajjad, U.; Yan, W.-M. A critical review on heat transfer augmentation of phase change materials embedded with porous materials/foams. *Int. J. Heat Mass Transf.* **2019**, *135*, 649–673. [CrossRef]
16. Al-Absi, Z.A.A.S.; Isa, M.H.M.; Ismail, M. Application of Phase Change Materials (PCMs) in Building Walls: A Review. In *The Advances in Civil Engineering Materials*; Awang, M., Isa, M.H., Eds.; Springer: Singapore, 2019; pp. 73–82.
17. Hoffmann, S. Numerische und Experimentelle Untersuchung von Phasenübergangsmaterialien zur Reduktion hoher Sommerlicher Raumtemperaturen. Ph.D. Thesis, Bauhaus-Universität Weimar, Germany, 2007.
18. Rida, M.; Hoffmann, S. The influence of macro-encapsulated PCM panel's geometry on heat transfer in a ceiling application. *Adv. Build. Energy Res.* **2021**, 1–21. [CrossRef]
19. Nazi, W.I.W.M.; Wang, Y.; Chen, H.; Zhang, X.; Roskilly, A.P. Passive Cooling Using Phase Change Material and Insulation for High-rise Office Building in Tropical Climate. *Energy Procedia* **2017**, *142*, 2295–2302. [CrossRef]
20. Irsyad, M.; Harmen. Heat transfer characteristics of coconut oil as phase change material to room cooling application. *IOP Conf. Ser. Earth Environ. Sci.* **2017**, *60*, 12027. [CrossRef]
21. Wonorahardjo, S.; Sutjahja, I.; Kurnia, D.; Fahmi, Z.; Putri, W. Potential of Thermal Energy Storage Using Coconut Oil for Air Temperature Control. *Buildings* **2018**, *8*, 95. [CrossRef]
22. Chauhan, A.; Tyagi, V.V.; Anand, S.; Pandey, A.K.; Sari, A.; Al-Sulaiman, F.A. Energy Storage by PCM for Building Applications. In *Handbook of Energy Systems in Green Buildings*; Wang, R., Zhai, X., Eds.; Springer: New York, NY, USA, 2018; pp. 995–1023.
23. Boussaba, L.; Makhlouf, S.; Foufa, A.; Lefebvre, G.; Royon, L. Vegetable fat: A low-cost bio-based phase change material for thermal energy storage in buildings. *J. Build. Eng.* **2019**, *21*, 222–229. [CrossRef]
24. Emmanuel, O.A.; Kessington, O.O.; Mudiakeoghene, O.J. Biodegradation of Vegetable Oils: A Review. Available online: http://www.academicjournals.org/SRE (accessed on 20 September 2021).
25. Wonorahardjo, S.; Sutjahja, I.M.; Kurnia, D. Potential of Coconut Oil for Temperature Regulation in Tropical Houses. *J. Eng. Phys. Thermophys.* **2019**, *92*, 80–88. [CrossRef]
26. Bulaka, B.; Syarifuddin, S.; Harianto, E. Coconut Oil Heat Capacity. *Prism. Sains J. Pengkaj. Ilmu Pembelajaran Mat. IPA IKIP Mataram* **2021**, *9*, 101–107.
27. Kahwaji, S.; White, M.A. Edible Oils as Practical Phase Change Materials for Thermal Energy Storage. *Appl. Sci.* **2019**, *9*, 1627. [CrossRef]
28. Khamooshi, A.; Kani, E.N. Development of a phase-change material for heat storage in gypsum-based building materials. In Proceedings of the Institution of Civil Engineers. *Energy* **2019**, *172*, 79–88.
29. Wi, S.; Seo, J.; Jeong, S.-G.; Chang, S.J.; Kang, Y.; Kim, S. Thermal properties of shape-stabilized phase change materials using fatty acid ester and exfoliated graphite nanoplatelets for saving energy in buildings. *Sol. Energy Mater. Sol. Cells* **2015**, *143*, 168–173. [CrossRef]
30. Jeon, J.; Park, J.H.; Wi, S.; Yang, S.; Ok, Y.S.; Kim, S. Characterization of biocomposite using coconut oil impregnated biochar as latent heat storage insulation. *Chemosphere* **2019**, *236*, 124269. [CrossRef]
31. Kottek, M.; Grieser, J.; Beck, C.; Rudolf, B.; Rubel, F. World Map of the Köppen-Geiger climate classification updated. *Meteorol. Z.* **2006**, *15*, 259–263. [CrossRef]
32. Beck, H.E.; Zimmermann, N.E.; McVicar, T.R.; Vergopolan, N.; Berg, A.; Wood, E.F. Present and future Köppen-Geiger climate classification maps at 1-km resolution. *Sci. Data* **2018**, *5*, 180214. [CrossRef]
33. Richards, D.; Masoudi, M.; Oh, R.R.Y.; Yando, E.S.; Zhang, J.; Friess, D.A.; Grêt-Regamey, A.; Tan, P.Y.; Edwards, P.J. Global Variation in Climate, Human Development, and Population Density Has Implications for Urban Ecosystem Services. *Sustainability* **2019**, *11*, 6200. [CrossRef]
34. Lee, H.; Jeong, S.G.; Chang, S.J.; Kang, Y.; Wi, S.; Kim, S. Thermal performance evaluation of fatty acid ester and paraffin based mixed SSPCMs using exfoliated graphite nanoplatelets (xGnP). *Appl. Sci.* **2016**, *6*, 106. [CrossRef]

35. Al-Jethelah, M.; Ebadi, S.; Venkateshwar, K.; Tasnim, S.H.; Mahmud, S.; Dutta, A. Charging nanoparticle enhanced bio-based PCM in open cell metallic foams: An experimental investigation. *Appl. Therm. Eng.* **2019**, *148*, 1029–1042. [CrossRef]
36. Alomair, M.; Alomair, Y.; Tasnim, S.; Mahmud, S.; Abdullah, H. Analyses of Bio-Based Nano-PCM filled Concentric Cylindrical Energy Storage System in Vertical Orientation. *J. Energy Storage* **2018**, *20*, 380–394. [CrossRef]
37. Ebadi, S.; Tasnim, S.H.; Aliabadi, A.A.; Mahmud, S. Geometry and nanoparticle loading effects on the bio-based nano-PCM filled cylindrical thermal energy storage system. *Appl. Therm. Eng.* **2018**, *141*, 724–740. [CrossRef]
38. Clarke, J.A. *Energy Simulation in Building Design*; Butterworth-Heinemann: Oxford, UK, 2001.
39. Yabuki, M.Y.; Otoni, C.; Celani, M.G.C. Alta tecnologia e reúso de materiais descartados: Desenvolvimento de um painel decorativo para a melhoria do desempenho térmico em edificações. *Gestão Tecnol. Proj.* **2020**, *15*, 6–19. [CrossRef]
40. Kenzhekhanov, S.; Memon, S.A.; Adilkhanova, I. Quantitative evaluation of thermal performance and energy saving potential of the building integrated with PCM in a subarctic climate. *Energy* **2020**, *192*, 116607. [CrossRef]
41. FAOSTAT: Top 10 Country Production of Coconuts 2019. Countries by commodity. Available online: http://www.fao.org/faostat/en/#rankings/countries_by_commodity (accessed on 20 September 2021).